Iron overload induced death of osteoblasts in vitro: involvement of the mitochondrial apoptotic pathway

Qing Tian [1], Shilei Wu [1], Zhipeng Dai [2], Jingjing Yang [3], Jin Zheng [4], Qixin Zheng [Corresp., 1], Yong Liu [Corresp. 1]

[1] Department of Orthopedics, Union Hospital, Tongji Medical College, Huazhong University of Science and Technology, Wuhan, Republic of China

[2] Department of Orthopedics, Henan Provincial People's Hospital, Zhengzhou, Republic of China

[3] Department of Child Health, Changzhou Maternal and Child Health Care Hospital, Changzhou, Republic of China

[4] Department of Neurology, Union Hospital, Tongji Medical College, Huazhong University of Science and Technology, Wuhan, Republic of China

Corresponding Authors: Qixin Zheng, Yong Liu
Email address: zheng-qx@163.com, 573846007@qq.com

Background. Iron overload isrecognized as a new pathogenfor osteoporosis. Various studies demonstrated that iron overload could induce apoptosis in osteoblasts and osteoporosis in vivo. However, the exact molecular mechanisms involved in the iron overload-mediated induction of apoptosis in osteoblasts has not been explored.

Purpose. In this study, we attempted to determine whether the mitochondrial apoptotic pathway is involved in iron-induced osteoblastic cell death and to investigate the beneficial effect of N-acetyl-cysteine (NAC) in iron-induced cytotoxicity.

Methods. The MC3T3-E1 osteoblastic cell line was treated with various concentrations of ferric ion in the absence or presence of NAC, and intracellular iron, cell viability, reactive oxygen species, functionand morphology changes of mitochondria and mitochondrial apoptosis related key indicators were detected by commercial kits. In addition , to further explain potential mechanisms underlying iron overload-related osteoporosis, we also assessed cell viability, apoptosis, and osteogenic differentiation potential in bone marrow-derived mesenchymal stemcells(MSCs) by commercial kits.

Results. Ferric ion demonstrated concentration-dependent cytotoxic effects on osteoblasts. After incubation with iron, an elevation of intracelluar labile iron levels and a concomitant over-generation of reactive oxygen species (ROS) were detected by flow cytometry in osteoblasts. Nox4 (NADPH oxidase 4), an important ROS producer, was also evaluated by western blot. Apoptosis, which was evaluated by Annexin V/propidium iodide staining, Hoechst 33258 staining, and the activation of caspase-3, was detected after exposure to iron. Iron contributed to the permeabilizatio of mitochondria, leading to the release of cytochrome C (cyto C), which, in turn, induced mitochondrial apoptosis in osteoblasts via activation of Caspase-3, up-regulation of Bax, and down-regulation of Bcl-2. NAC could reverse iron-mediated mitochondrial dysfunction and blocked the apoptotic events through inhibit the generation of ROS. In addition, iron could significantly promote apoptosis and suppress osteogenic differentiation and mineralization i n bone marrow-derived MSCs.

Conclusions. These findings firstly demonstrate that the mitochondrial apoptotic pathway involved in iron-induced osteoblast apoptosis. NAC could relieved the oxidative stress and shielded osteoblasts from apoptosis casused by iron-overload. We also reveal that iron overload in bone marrow-derived MSCs results in increased apoptosis and the impairment of osteogenesis and mineralization.

1 **Iron Overload Induced Death of Osteoblasts In Vitro: Involvement of**

2 **the Mitochondrial Apoptotic Pathway**

4 Qing Tian[1*],Shilei Wu[1*], Zhipeng Dai[2], Jingjing Yang[3], Jin Zheng[4], Qixin Zheng[1], Yong Liu[1]

5 [1] Department of Orthopedics, Union Hospital, Tongji Medical College, Huazhong University of

6 Science and Technology, Wuhan, Hubei, China

7 [2] Department of Orthopedics, Henan Provincial People's Hospital, Zhengzhou, Henan, China

8 [3] Department of Child Health, Changzhou Maternal and Child Health Care Hospital, Changzhou,

9 Jiangsu, China

10 [4] Department of Neurology, Union Hospital, Tongji Medical College, Huazhong University of

11 Science and Technology, Wuhan, Hubei, China

12 [*]These authors contributed equally to this work.

14 **Corresponding author**

15 Yong Liu (liuyongxiehexiqu@163.com)

16 Qixin Zheng (zheng-qx@163.com)

17 Department of Orthopedics, Union Hospital, Tongji Medical College, Huazhong University of

18   Science and Technology, Wuhan, Hubei, China

Abstract

Background. Iron overload is recognized as a new pathogen for osteoporosis. Various studies demonstrated that iron overload could induce apoptosis in osteoblasts and osteoporosis in vivo. However, the exact molecular mechanisms involved in the iron overload-mediated induction of apoptosis in osteoblasts has not been explored.

Purpose. In this study, we attempted to determine whether the mitochondrial apoptotic pathway is involved in iron-induced osteoblastic cell death and to investigate the beneficial effect of N-acetyl-cysteine (NAC) in iron-induced cytotoxicity.

Methods. The MC3T3-E1 osteoblastic cell line was treated with various concentrations of ferric ion in the absence or presence of NAC, and intracellular iron, cell viability, reactive oxygen species, function and morphology changes of mitochondria and mitochondrial apoptosis related key indicators were detected by commercial kits. In addition, to further explain potential mechanisms underlying iron overload-related osteoporosis, we also assessed cell viability, apoptosis, and osteogenic differentiation potential in bone marrow-derived mesenchymal stem cells (MSCs) by commercial kits.

Results. Ferric ion demonstrated concentration-dependent cytotoxic effects on osteoblasts. After incubation with iron, an elevation of intracelluar labile iron levels and a concomitant over-generation of reactive oxygen species (ROS) were detected by flow cytometry in osteoblasts. Nox4 (NADPH oxidase 4), an important ROS producer, was also evaluated by western blot.

40 Apoptosis, which was evaluated by Annexin V/propidium iodide staining, Hoechst 33258

41 staining, and the activation of caspase-3, was detected after exposure to iron. Iron contributed to

42 the permeabilizatio of mitochondria, leading to the release of cytochrome C (cyto C), which, in

43 turn, induced mitochondrial apoptosis in osteoblasts via activation of Caspase-3, up-regulation of

44 Bax, and down-regulation of Bcl-2. NAC could reverse iron-mediated mitochondrial dysfunction

45 and blocked the apoptotic events through inhibit the generation of ROS. In addition, iron could

46 significantly promote apoptosis and suppress osteogenic differentiation and mineralization in

47 bone marrow-derived MSCs.

48 **Conclusions.** These findings firstly demonstrate that the mitochondrial apoptotic pathway

49 involved in iron-induced osteoblast apoptosis. NAC could relieved the oxidative stress and

50 shielded osteoblasts from apoptosis casused by iron-overload. We also reveal that iron overload

51 in bone marrow-derived MSCs results in increased apoptosis and the impairment of osteogenesis

52 and mineralization.

54 **Introduction**

55   Iron is an essential element for several cellular and metabolic processes. However, this

56 transition metal also catalyzes the formation of damaging free radicals, leading to the oxidative

57 injury of cellular components. Osteoporosis and fractures occur frequently in patients with

58 disorders associated with iron overload such as thalassemia and hemochromatosis *(Vogiatzi MG*

59 *et al., 2006; Vogiatzi MG et al., 2009; Kim BJ et al., 2012; Wong P et al., 2014)*. Evidence from

60 numerous studies indicates that iron overload directly exerts detrimental effects on bone

61 metabolism *(Yang Q et al., 2011; Tsay J et al., 2010)*. Excessive iron accumulation in osteoblast

62 triggers apoptosis which may play essential roles in osteoporosis *(Messer JG et al., 2009;*

63 *Doyard M et al., 2012)*. However, the mechanism by which iron induces apoptosis is not fully

64 understood. Therefore, the elucidation of the mechanisms underlying apoptosis and development

65 of therapeutic strategies to block apoptosis in osteoblasts are crucial for treating iron-overload

66 induced osteoporosis.

67   Apoptosis occurs via two major pathways: the death receptor pathway and mitochondrial

68 pathway. The death receptor pathway is mainly initiated by the ligation of death receptors such

69 as tumor necrosis factor (TNF) and Fas/CD95, in which the recruited caspase 8 acts as a trigger

70 for the activation of caspase 3 and apoptosis *(Fuchs Y et al., 2011)*. The mitochondrial pathway,

71 known as another important apoptotic pathway, is activated by various stimuli that induce the

72 dissipation of the mitochondrial membrane and the release of apoptotic factors such as cyto *c*

73 *(Kroemer G et al., 2007; Green DR et al., 2014)*. After cyto c is released into the cytosol, its

74   initiates the formation of cytochrome c /Apaf-1/ Caspase-9 complex (termed the apoptosome),

75   which causes the activation of Caspase-3, subsequently executing cell apoptosis *(Tait SW et al.,*

76   *2013)* . However, the specific apoptotic pathway by which iron induces apoptosis in osteoblasts

77   has not been reported.

78   Studies have confirmed that redox-active iron in mitochondria is capable of directly

79   catalyzing the formation of deterimental free radicals via Fenton chemistry *(Lill R., 2009; Dixon*

80   *SJ et al., 2014)*. Both iron-dependent ROS and high concentrations of labile iron are thought to

81   contribute to mitochondrial ultrastructural damage *(Pietrangelo A et al., 2016)* . Therefore, we

82   hypothesize that iron-induced osteoblast apoptosis may be mediated by the mitochondrial

83   apoptotic pathway. Furthermore, we explored the role of the mitochondrial pathway in iron-

84   overload induced osteoblast apoptosis by examining mitochondrial function and apoptosis

85   related key molecules. In additon, in our present study, the protection of NAC on iron overload-

86   induced osteoblasts apoptosis has been investigate.

87

Materials & Methods

Materials

90   N-acetyl-cysteine (NAC), Ferric ammonium citrate (FAC), 2',7'-dichlorodihy-

91   drofluorescein diacetate (H2DCF-DA), calcein-AM, Hoechst33258, 4',6-diamidino-2-

92   phenylindol (DAPI), penicillin, streptomycin, leupeptin, pepstatin A, deaprotinin,

93 phenylmethylsulfonylfluoride (PMSF), and 4-(2-hydroxyethyl)-1-piperazineethane sulfonic acid

94 (HEPES) were purchased from Sigma (USA). Primary antibodies against cytochrome c, bcl-2,

95 bax, cleaved Caspase-3, Glyceraldehyde-3-Phosphate Dehydrogenase (GAPDH) and beta-actin

96 (β-actin) were purchased from Abcam (UK). AnnexinV–FITC/PI kit was obtained from KeyGen

97 Biotech (China). Fetal bovine serum and alpha-modified Eagle's medium (a-MEM) were

98 purchased from Gibco (USA). Cell Mitochondria Isolation Kit, Enhanced Chemiluminescence

99 detection kit, Western and immunoprecipitation (IP) Cell Lysis Kit, Bicinchoninic Acid Protein

100 (BCA) Protein Assay Kit, and 5,5',6,6'-tetrachloro-1,1',3,3'-

101 tetraethylbenzimidazolcarbocyanineiodide (JC-1) were purchased from Beyotime (China). Cell

102 Counting Kit-8 (CCK-8) assay kit was purchased from DojinDo (Japan).

103 **Cell cultures and treatment**

104 MC3T3-E1 osteoblasts (obtained from American Type Culture Collection) were cultured in

105 alpha-modified Eagle's medium supplemented with 10% fetal bovine serum (FBS) (Gibco H,

106 Invitrogen, Grand Island, NY, USA), 50 U/ml penicillin, and 50 mg/ml streptomycin. The

107 medium was changed thrice one week. Cells were cultured to 80-90% confluence, harvested ,

108 and seeded at 1×10^4 cell/cm^2 in 96- and 6-well plates.

109 FAC, which functions as an iron donor, was used to simulate iron overload conditions in

110 vitro *(Doyard M et al., 2012; Zarjou A et al., 201*0). We incubated MC3T3-E1 cells with various

111 concentrations of FAC: 25, 50, 100, and 200 μM. Control groups were treated with PBS. After

112 exposure to FAC in the absence or presence of NAC (1mM), all samples were collected

113   subsequent analyses by flow cytometry, Western Blot, confocal microscopy, and fluorescence

114   microscopy.

115   Primary bone marrow-derived MSCs were isolated from Sprague-Dawley rats (100–120 g,

116   obtained from the Animal Center of Tong Ji Medical College, Huazhong University of Science

117   and Technology) as previously described *(Meng J et al., 2016)*. The isolated cells were cultured

118   in 55-m^2 dishes in Dulbecco's modified Eagle's medium (HyClone, USA) with 10% (v/v) fetal

119   bovine serum (FBS) and 100 μg/mL streptomycin and penicillin(Beyotime-biotechnology, China)

120   at 37℃, 5% CO_2 atmosphere. The growth medium was changed every 2 days. Primary bone

121   marrow-derived MSCs were grown to confluence and used from passages 3 to 6 throughout the

122   following experiments.

123   **Measurement of cell viability**

124   The cell counting kit-8 was applied to determine viability of osteoblastic cells and bone

125   marrow-derived MSCs as described previously*(Ding F et al., 2012; Cai XY et al., 2015)*. After

126   exposure to FAC (25-200 μM) for 24 and 120 h, the mixture solution containing medium (90 μl)

127   and CCK-8 reactant (10 μl) was added to each well of a 96- well plate. Then, the sample was

128   incubated at 37°C for 2 h in the dark. Finally, the absorbance at 450 nm was analyzed in a

129   spectrophotometer (Thermo, USA).

130   **Assay of the intracellular labile iron level by flow cytometry and fluorescence microscopy**

131   The labile iron pool (LIP), which refers to the level of intracellular redox-active and

132 chelatable iron, has been implicated in cellular damage by catalyzing excess-production of

133 deterimental free radical. The intracellular LIP was measured by flow cytometry following

134 calcein staining. Briefly, after treatment with FAC (0–200 µM) for 120 h, the osteoblasts were

135 collected and resuspended in PBS, and subsequently treated with 0.25 µM calcein-AM in dark at

136 37°C for 30 min *(Tenopoulou M et al., 2007; Glickstein H et al., 2005; Kaur D et al., 2008)*.

137 Next, osteoblasts were rinsed twice with serum-free a-MEM, gently resuspended in the medium,

138 and immediately analyzed by flow cytometry using CellQuest analysis software (BD Biosciences,

139 USA). Meanwhile, in order to evaluate the change in intracellular labile iron levels in situ, all

140 samples were additionally monitored under a fluorescence microscope.

141 **Evaluation of intracellular reactive oxygen species**

142 Levels of ROS in osteoblasts were determined with H2DCF-DA, a fluorescent dye, which

143 could be rapidly oxidized into the highly fluorescent compound DCF in the presence of ROS

144 *(Ma KG et al., 2013)*. Following treatment with FAC, the osteoblasts were collected and washed

145 with PBS, subsequently resuspended in serum-free media, and finally treated with 20 µM

146 H2DCF-DA in dark at 37°C for 20 min *(Ding F et al., 2012)*. After incubation, MC3T3-E1 cells

147 were rinsed with serum-free a-MEM thrice, and subsequently the mean fluorescence intensity

148 (MFI) was evaluated with a FACSCalibur flow cytometer (BD, USA).

149 **Evaluation of apoptosis by Annexin V-FITC/PI staining**

150 After treatment as described above, osteoblasts and bone marrow-derived MSCs from each

151   sample were stained using the Annexin V–FITC/PI kit, as described previously *(Ding F et al.,*

152   *2012; Cai XY et al., 2015)*. Then, flow cytometry was accomplished by flow cytometric

153   analysis (BD, USA). The sample was additionally visualized under a confocal microscope

154   (OLYMPUS FV1000, Japan). The Annexin V+/PI- osteoblasts were

155   considered early apoptotic cells *(Henry CM et al., 2013)*. The Annexin V+/PI+ osteoblasts were

156   considered late apoptotic cells *(Henry CM et al., 2013)* .

157   **Evaluation of apoptosis-related morphologic changes in osteoblasts**

158   To verify apoptosis, ding (*Ding F et al., 2012; Cai XY et al., 2015*) outlined a procedure for

159   ascertaining apoptosis, through the application of Hoechst 33258 dye at 0.5 μg/mL concentrate,

160   to clarify the fractured and compressed apoptotic nuclei. Following the application of the dye,

161   the nuclei were stained for one hour at 37°C with all light sources omitted. The nuclei were then

162   given two washes with PBS, so as to remove the Hoechst 33258. Utilising a fluorescence

163   microscope manufactured by Carl Zeiss, the morphology of osteoblast apoptosis was pictured

164   with UV excitation at 350nm, then analysed.

165   **Measurement of mitochondrial membrane potential (MMP)**

166   The collapsed MMP in osteoblasts was detected by flow cytometry following JC-1 dye

167   staining (Beyotime-biotechnology, China). Briefly, after treatment as described above, the

168   harvested MC3T3-E1 cells were resuspended in a staining solution, which were prepared by

169   admixing serum-free a-MEM (500 μL) and JC-1 staining fluid (500 μL). Subsequently,

170 osteoblasts were incubated with the staining solution for 20 min at 37°C in the dark. After

171 incubation, osteoblasts were washed thrice with the JC-1 staining buffer (Beyotime-

172 biotechnology, China), and resuspended in 500 μL of cell culture medium prior to analysis by

173 flow cytometry. Finally, the ratio of red fluorescence intensity to green fluorescence intensity

174 was calculated, and the results were used to evaluate the change in MMP for each sample*(Ding F*

175 *et al., 2012)*.

176   In order to evaluate the change in MMP in situ, osteoblasts were loaded with JC-1 dye after

177 treatment with FAC, as described above *(Ding F et al., 2012)*. Aggregated JC-1 (red

178 fluorescence) and monomeric JC-1 (green fluorescence) levels were observed using laser

179 scanning confocal microscopy (Olympus FV1000, Japan).

180 **Western blot analysis**

181   After treatment with FAC, as described above, osteoblasts were collected and homogenized

182 in lysis buffer. The details of the Western blotting procedures have been described previously

183 *(Ding F et al., 2012)*. The monoclonal antibodies used were as follows: anti-cleaved Caspase-3

184 (1 : 2000), anti-Bax (1 : 1000), anti-Bcl-2 (1 : 1000), and anti-Cytochrome c (1 : 1000). GAPDH

185 and beta-actin were utilized as internal controls.

186 **Induction of osteogenic differentiation of bone marrow-derived MSCs and Alizarin Red**

187 **staining**

188   To detect the iron effect on osteogenic differentiation, Cyagen® osteogenesis differentiation

189 medium (Cyagen Biosciences., China) were used following the manufacturer's protocol *(Zhu Y*

190 *et al., 2012)*. Briefly, primary bone marrow-derived MSCs were cultured in osteogenesis

191 differentiation media (2 mmol/L β-glycerol-phosphate, 50 μmol/L ascorbic acid, 0.1 μmol/L

192 dexamethasone) alone or in the presence of FAC for 14 days. After induction, osteogenesis was

193 eveluated by staining MSCs with Alizarin Red S reagent (Cyagen Biosciences., China) as

194 protocol described.

195 **Evaluation of the deposition of calcium**

196   Primary bone marrow-derived MSCs were subcultured in 6-well plates in growth medium

197 (Dulbecco's modified Eagle's medium, 10% fetal bovine serum (FBS) and 100 lg/mL

198 streptomycin and penicillin). After primary bone marrow-derived MSCs had reached

199 approximately 80% confluence, FAC was added to the osteogenesis differentiation medium. To

200 quantify the iron effect on the matrix calcification, Alizarin red S staining were used following

201 the manufacturer's protocol *(Zhang X et al., 2010)*. Positive red staining represents calcium

202 deposits of on the differentiated MSCs. For quantification of staining, 100 mM cetypyridinium

203 chloride was added to each plate and used to extracte Alizarin red S, and the sample was

204 incubated at room temperature for 3 h *(Malladi P et al., 2006)*. Finally, the absorbance of the

205 extracted Alizarin red S at 570 nm was analyzed in a spectrophotometer (Thermo, USA).

206 **Measurement of Alkaline phosphatase activity (ALP)**

207   Primary bone marrow-derived MSCs treated on 6-well plates were rinsed with PBS thrice,

208   lysed in RIPA solution (Beyotime-biotechnology, China), and finally centrifuged to remove

209   cellular debris at 4℃. Next, ALP activity in the samples was measured by p-nitrophenyl

210   phosphate method using a Alkaline Phosphatase Assay Kit (Beyotime-biotechnology, China) as

211   previous report *(Lyu Z et al., 2014)*.

212   **Statistical analysis**

213   All data were expressed as means ± standard

214   deviation(SD).Statistical analyses were performed with SPSS software (version 18.0) for

215   Windows software. In order to analyze statistical differences between samples, we used one-

216   way analysis of variance (ANOVA) with least significant difference (LSD). $P < 0.05$ was

217   considered statistically significant.

218

219   # Results

220   **Influences of iron on osteoblastic cell viability**

221   In our present study, the CCK-8 assay kit results indicated that iron had toxic effects. After

222   a 120-h exposure to FAC, the viability of osteoblasts was found to be significantly inhibited by

223   iron in a dose-dependent manner. However, after a 24-h exposure to FAC, no statistically

224   significant difference was observed between the viability of osteoblasts at the various

225   concentrations tested[Fig.1]. These results imply that iron may undergo accumulation in

226   osteoblasts ,which may elicit cytotoxic effects in these cells.

227 Increase in intracellular labile iron levels due to iron overload in osteoblasts

228   Labile iron pool, known as free and chelatable iron, is the major potentially toxic form in

229 iron-overload related diseases *(Brissot P et al., 2011)*. To evaluate changes of LIP in osteoblasts,

230 a fluorescent iron-sensitive probe, calcein-AM was used. When calcein-AM permeates into the

231 osteoblast and binds the intracellular labile iron, its fluorescence is quenched enabling evaluation

232 of the intracellular labile iron levels by via measurement of the decrease in calcein-AM

233 fluorescence *(Tenopoulou M et al., 2007; Glickstein H et al., 2005; Kaur D et al., 2008)*. After

234 incubation with FAC (25-200 μM) for 120 h, the mean fluorescence intensity of calcein-AM

235 decreased in a dose-dependent manner, which indicated a significant increase in the intracellular

236 labile iron levels within the osteoblasts [Fig. 2].

237 Impacts of iron on ROS level and expression of NADPH oxidase 4 (Nox4) in osteoblasts

238   To determine whether the over-production of ROS plays a pivotal role in iron-induced

239 apoptosis, we used the specific fluorescence dye, H2DCF-DA, which detected intracellular ROS

240 formation. According to the results of H2DCF-DA staining, a concentration-dependent increase

241 in intracellular ROS production was observed in osteoblasts exposed to various concentrations of

242 FAC (25-200 μM) for 120 h [Fig. 3] ; the ROS levels were found to be 1.82- ,4.00- , 7.75- , and

243 10.55-fold higher after treatment of osteoblast with 25, 50, 100, and 200 μM FAC, respectively

244 [Fig. 3(B)]. NADPH oxidase is one of the most important ROS producers within the cell *(Sahoo*

245 *S et al., 2016)*. In our study, we determined that FAC affects expression of Nox4, which mainly

246 mediates the clinical phenotype in bone loss-related diseases *(Manolagas SC et al., 2010;*

247   *Schröder K et al., 2015).* Our results indicate that FAC (25-200 μM) upregulates Nox4 in

248   osteoblasts.

249   **Effects of iron on apoptosis in osteoblasts**

250   In order to assess whether iron mediated toxicity in osteoblasts is related to the activation of

251   apoptosis, a following investigation was made. Annexin V/PI apoptosis assay kit were used to

252   evlaute the apoptosis rate of osteoblasts. Annexin V+/PI- osteoblasts and Annexin+/PI+

253   osteoblasts were considered apoptotic cells. Following the application of FAC for 120 h at 0, 25,

254   50, 100 and 200 μM, apoptosis was seen to raise from 4.41% to 56.72%, as illustrated by [Fig.

255   4(B)]. Furthermore, compared to control group (FAC 0 μM), there was a mainly raised amount

256   of late apoptosis after FAC (200 μM) expouse in [Fig. 4(A)], with [Fig. 4(C)] also suggestive of

257   a similar impact in osteoblasts.

258   Phase-contrast microscopy and fluorescence microscopy were also utilised to observe the

259   morphology of osteoblasts and the degree of apoptosis resulting from iron exposure. The resluts

260   of nuclear-staining with Hoechst indicated that, compared to 0 μM FAC (control), the proportion

261   of osteoblasts with condensed or fragmented nuclei markedly increased in the FAC treatment

262   group [Fig. 5(A)]. Phase-contrast microscopy indicated that osteoblasts incubated with FAC (200

263   μM) for 120 h revealed apoptosis-related morphology, characterized by cell shrinkage, rounding

264   and floating in 6-well plates [Fig. 5(B)].

265   **Involvement of cleaved Caspase-3, cytochrome c, Bax and Bcl-2 in iron-induced apoptosis**

266   In order to confirm that the mitochondrial pathway associated with iron treatment, we

267 detected the release of cytochrome c into cytoplasm and the generation of cleaved Caspase-3 by

268 Western blot. As illustrated by [Fig. 6], after FAC (25-200 μM) treatment for 120 h, a dose-

269 dependent up-regulation of cytochrome c in this study was detected, which was accompanied by

270 the generation of activated fragments of Caspase-3.

271   To investigate whether iron induces osteoblast apoptosis through alterations in Bcl-2 and

272 Bax expression, Western blot were utilized to analyze Bax and Bcl-2 protein levels. In our

273 present experiment, a dose-dependent down-regulation of Bcl-2, as well as an up-regulation of

274 Bax was observed in osteoblasts exposed to FAC (25-200 μM) for 120 h [Fig. 6].

275 **Depolarisation of MMP in osteoblasts due to iron**

276   Apoptosis could be initiated by the reduction of MMP, therefore it was decided to

277 investigate whether such a reduction of MMP and consequent apoptosis is induced by iron. JC-1

278 dying of the osteoblasts and a flow cytometry were utilised to assess the amount of MMP. [Fig.7]

279 shows how MMP was diminished with the application of FAC in various quantities for 120 h.

280 An increase in the strength of fluorescence of green JC-1 monomers compared to red JC-1

281 aggregates was considered to signify a significant reduction in MMP. [Fig. 7(C)] illustrates how

282 the control group's MMP had no reduction following JC-1 dying, due to apparent diminished

283 strength of green fluorescence compared to red fluorescence. However, a breakdown of MMP

284 was seen to be associated with apoptotic osteoblasts caused by increased iron levels. An

285 increased number of mitochondria were observed with a greater amount of green fluorescence,

286   following the addition of FAC at varying concentrations of 25- 200 µM, for a duration of 120 h.

N-acetyl-L-cysteine (NAC)'s protection impact on iron-related apoptosis in osteoblasts

288   This was to ascertain the extent to which NAC can prevent apoptotic occurrences related to

289   iron in osteoblasts, by reducing the creation of ROS. The results suggested that the application of

290   NAC was able to reduce the mitochondria's loss of cytochrome c, reduce the creation of ROS as

291   an effect of iron to a large degree and consequently diminish the breakdown of MMP related to

292   iron [Fig. 8]. As illustrated by [Fig. 8(E)], Caspase-3's stimulation was thus inhibited by NAC,

293   Bcl-2/Bax modulation was inverted, while apoptotic osteoblasts resulting from the effects of iron

294   were effectively reduced by NAC's application to osteoblasts. Therefore, apoptosis as a result of

295   the effects of iron can also be seen to be significantly exacerbated by ROS production.

Effects of iron on bone marrow-derived MSCs viability and apoptosis

297   MSCs, characterised by their multipotent differentiation capacity, are recruited to the

298   bone remodeling surface and differentiated into osteoblasts, which play an essential role to

299   maintain bone mass. To test the effects of iron on the viability of MSCs in vitro, the CCK-8

300   assay kit was used in our study. As shown in [Fig. 9], iron inhibited the viability of MSCs at 72 h

301   and 144 h in a dose-dependent manner. Next, we detected whether apoptosis was involved in

302   iron-induced cellular toxicity. As reported in [Fig. 10], a significant increase of the apoptosis

303   rates was observed in bone marrow-derived MSCs exposed with FAC (200 µM) for 144 h. Taken

304   together, iron overload- induced toxicity of bone marrow-derived MSCs appears to be partially

305   mediated by apoptosis.

306   **Inhibitory effects of iron on osteogenic differentiation and mineralization**

307   To investigate whether excess iron impaire osteogenesis of bone marrow-derived MSCs and

308   mineralization, cells were cultured in osteogenesis differentiation media alone or in the presence

309   of FAC (25- 200 μM) for 14 days. Next, the activity of ALP, a specific marker of osteogenic

310   differentiation, was detected in bone marrow-derived MSCs. [Fig. 11(A)] shows that iron caused

311   a concentration-dependent inhibitory effect of the activity of ALP in osteogenesis of MSCs. In

312   addtion, Alizarin Red staining showed that iron leaded to a concentration-dependent impairment

313   of mineralization. At the concentration of 200μM, iron almost completely inhibited the

314   mineralization process of MSCs in vitro. Then, we estimated the effect of iron-overload on

315   calcium deposotion of the extracellular matrix. As demonstrated in [Fig. 11(B-D)], FAC caused a

316   decrease in the calcium content of the extracellular matrix in a dose-dependent manner,

317   which is accordance with the Alizarin Red staining results.

318

319   **Discussion**

320   Osteoporosis has been reported to be closely related with iron overload, which may arise

321   due to conditions such as hemochromatosis and the thalassemia *(Wong P et al., 2013; Haidar R*

322   *et al., 2011; Valenti L et al., 2009)*. Meanwhile, various studies confirmed that age-associated

323   iron accumulation is a contributing factor in the pathogenesis of postmenopausal osteoporosis

324   *(Li GF et al., 2012; Fiona Mitchell et al., 2012)*. It has also been demonstrated that increased

325   physiological iron stores could accelerate bone loss, even in healthy adults *(Kim BJ et al., 2012;*

326   *Fiona Mitchell et al., 2012)*. The maintenance of normal skeletal homeostasis relies on

327   osteoblasts, which is responsible for bone matrix synthesis, secretion and mineralization. The

328   impairment of osteoblasts is considered to be a major factor contributing to osteoporosis in iron

329   overload related diseases *(Domrongkitchaiporn S et al., 2003; Terpos E et al., 2010;*

330   *Mahachoklertwattana P et al., 2003; Doyard M et al., 2016)*. Therefore, it is essential to

331   investigate the toxic effects of iron on osteoblasts and elucidate the molecular mechanisms of

332   iron toxicity in these cells. Our present experiment reveals that iron-overload causes deterimental

333   effects in the osteoblastic cellular proliferation. We have also found that iron-overload

334   effectively induces apoptosis in osteoblasts in vitro, which is in accordance with the findings of

335   previously published research *(Messer JG et al., 2009; Doyard M et al., 2012)*. More

336   interestingly, our study, for the first time, suggests that the apoptosis caused by iron overload is

337   correlated with activation of the mitochondrial pathway.

338   While iron is a fundamental element for various crucial biological processes, such as

339   enzymatic reactions and oxygen transport, excess iron accumulation could damge cells by

340   catalyzing the over-production of damaging hydroxy radical through Haber–Weiss reactions

341   *(Dixon SJ et al., 2014)*. Labile iron pool, known as free and chelatable iron, is the major

342   potentially toxic form in iron-overload related diseases *(Esposito BP et al., 2003; Devos D et al.,*

343   *2014; Berdoukas V et al., 2015; Chai X et al., 2015)*. In this study, we observed that the

344   intracellular LIP level in osteoblasts was significantly increased after exposure to FAC for 120 h.

345   ROS, which induced by labile iron via iron-dependent oxidase (for example, xanthine oxidase,

346   nicotinamide adenine dinucleotide phosphate hydride oxidases, lipoxygenases) or the Haber–

347   Weiss reaction, is primary responsible for cellular damage caused by iron overload *(Dixon SJ et*

348   *al., 2014)*. Numerous studies reported that celluar and genomic oxidative damage were highly

349   correlated with elevated levels of labile iron in thalassemia patients *(Brissot P et al., 2012;*

350   *Berdoukas V et al., 2015)*. Next, we evaluated the generation of ROS in osteoblasts after

351   exposure to FAC and found that iron-overload induced ROS production drastically increased.

352   Moreover, the over-production ROS was paralleled with the increase of intracellular labile iron

353   and the cytotoxicity of osteoblasts. The generation of ROS is tightly regulated through various

354   ways, including NADPH oxidases, phagocyte oxidase and mitochondrial electron transport chain

355   *(Sahoo S et al., 2016; Dikalov S et al., 2011; Zhou J et al., 2013)*. Emerging evidence indicates

356   that NADPH oxidases are the primary generator of ROS in the skeletal system and Nox-derived

357   ROS are key players which mediates osteoblasts dysfunction with osteoporosis *(Manolagas SC*

358   *et al., 2010; Schröder K et al., 2015)*. In our study, we found that iron overload could upregulate

359   the expression of NADPH oxidase 4 (Nox4) in osteoblasts after treatment with FAC. In addition,

360   heme (an iron derivative), as electron transporter, plays an important role for superoxide

361   generation of NOX family NADPH oxidases *(Bedard K et al., 2007)*.

362   Therefore, Nox4 may be an essential part in iron-overload induced generation

363   of ROS in osteoblasts.

364   Previous studies have also shown that iron overload exerts deterimental effects on various

365   cell types and its mechanisms by which iron toxicity occurs are closely associated with

366   apoptosis*(Chan S et al., 2013; Park J et al., 2015; Dussiot M et al., 2014)*. In this experiment, we

367   demonstrated that iron-overload effectively induced apoptosis in osteoblasts. Furthermore, the

368   activation of Caspase-3 was also observed after treatment with FAC. Although it is well

369   established that iron-overload could induce apoptosis, its exact pathway in osteoblasts is still

370   largely unknown. In iron-overload conditions, excess labile iron enters the mitochondria via the

371   calcium uniporter, and then interacts with reactive oxygen intermediates leaked from

372   mitochondrial respiratory chain through Fenton reactions, catalyzing powerful ROS to damage

373   mitochondria *(Chen MP et al., 2014; Sripetchwandee J et al., 2014; Pelizzoni I et al., 2011;*

374   *Uchiyama A et al., 2008)*. ROS catalyzed by labile iron elicits a range of detrimental effects in

375   mitochondria, as following (1) impairment of mitochondrial respiratory enzyme activity; (2)

376   decrease in ATP production; (3) loss of MMP; and (4) damage to mitochondrial DNA (mtDNA)

377   *(Ward RJ et al., 2014; Mallikarjun V et al., 2014; Al-Qenaei A et al., 2014; Santambrogio P et*

378   *al., 2015; Rouault TA., 2016; Rines AK, Ardehali H. 2013)*. In this experiment, the inhibition of

379   mitochondrial dehydrogenase activity was observed in osteoblasts exposed to FAC. Considering

380   that ROS enhanced by iron overload could impair mitochondrial ultrastructure and disrupt its

381   function, which might subsequently activate Caspase-3 through various molecular cascade

382   reactions, we hypothesized that iron-overload induced apoptosis of osteoblasts might occur

383   through the mitochondrial pathway.

384   The mitochondrial apoptosis pathway has been well documented by many previous studies

385   *(Czabotar PE et al., 2014)*. In the mitochondrial pathway, mitochondrial membrane

386   permeabilization, characterized by the loss of MMP, is considered as the most critical event

387   activating caspase and causes apoptosis *(Fuchs Y et al., 2011; Kroemer G et al., 2007)*. After

388   mitochondrial membrane permeabilization induced by various apoptotic stimuli, Cyto c releases

389   from mitochondrial intermembrane space, subsequently binds APDF1 in cytosol, and then forms

390   apoptosome through recruiting and activating caspase 9. Eventually, caspase-9 cleaves and

391   activates caspase-3, resulting in the activation of apoptotic cell death *(Fuchs Y et al., 2011;*

392   *Kroemer G et al., 2007)*. Therefore, the changes of MMP in osteoblasts after treatment with FAC

393   were studied in details. Confocal microscopy observation indicated that iron overload led to a

394   dose-dependent decrease of MMP in osteoblasts. Furthermore, the depolarization of MMP was

395   subsequent accompanied with Cyto C release from mitochondria into the cytoplasm. Based on

396   above data, we then further to study the expression changes of other essential molecules

397   regulating the mitochondrial apoptosis pathway to prove our hypothesis. Bcl-2 family proteins

398   have been confirmed to control cellular apoptosis by directly or indirectly regulating

399   mitochondrial membrane permeabilization *(Czabotar PE et al., 2014)*. Bcl-2, an anti-apoptotic

400   molecule, and Bax, an pro-apoptotic molecule, are key members among the Bcl-2 family

401   *(Hardwick JM et al., 2013)*. The decrease in Bcl-2 or increase in Bax, could promote

402   permeabilization of the mitochondrial membrane, leading to the release of Cyto c and eventually

403   triggering apoptosis*(Kroemer G et al., 2007)*. In our study, we observed that iron overload

404   caused the upregulation of Bax and cleaved caspase-3, as well as the downregulation of Bcl-2.

405   The changes of Bcl-2 and Bax expression in osteoblasts may have been suffcient to facilitate

406   mitchondrial membrane permeability. Taken together, our findings indicate that the

407   mitochondrial apoptosis pathway might be invovled, at least in part, in iron overload-related

408   osteoblast injury.

409   NAC is a well-known antioxidant, which elevates the intracellular glutathione levels, an

410   important module in the cellular antioxidative system *(Tsay J et al., 2010)*. In our study, we

411   found that apoptosis induced by iron overload in osteoblasts was associated with increased

412   harmful free radicals and was also largely prevented by NAC. Meanwhile, previous studies also

413   found that NAC could enhance osteogenesis and inhibit osteoclast differentiation *(Yamada M et*

414   *al., 2013; Jun JH et al., 2008; Hyeon S et al., 2013; Lee NK et al., 2005)*. This suggests that

415   NAC could be an adjunctive therapy in iron-overload related bone loss. The concept that

416   increased harmful free radicals induced by iron overload is the main contributer of iron toxicity

417   is not new. But, to our knowledge, detailed mechanism for NAC protection against iron

418   overload-induced osteoblasts apoptosis has not been reported. Our findings revealed that NAC

419   could prevent the mitochondria damage casused by iron overload through directly scavenge the

420   over-generated ROS. Thus, cytochrome c released from mitochondria was decrease and the the

421   activation of caspase-3 was inhibited. In addition, after NAC treatment, the expression of Bcl-2

422   was markedly increase, while the expression of Bax was decrease. This result might imply that

423   Bcl-2 family proteins also involved in the NAC protection effects.

424   Our study was highly reproducible; however, some limitations should be noted. Firstly, our

425   studies were conducted in vitro; as such our results may not be representative of biological

426   process in vivo. Furthermore, as human osteoblastic cells are difficult to obtain, we utilized the

427   MC3T3-E1 osteoblastic cell line to examine the toxicity of iron in this study. Although

428   numerous studies have reported that the MC3T3-E1 cell line is similar to human osteoblasts in

429   function*(Czekanska EM et al., 2012)*, further studies using human osteoblasts are warranted.

430   Finally, our results indicate that the mitochondrial apoptotic pathway is involved in mediating

431   iron toxicity in osteoblasts. However, the iron-mediated destabilization of lysosomal membranes

432   represents an alternative mechanism of iron toxicity. In future experiments, we aim to explore

433   the potential effects of iron on lysosomes, which may include, lysosomal membrane

434   permeabilization and cross-talk between lysosomes and mitochondria.

435   In the maintenance of skeletal homeostasis, besides osteoblast, mesenchymal stem cell also

436   also plays an essential role in osteogensis. It has been reported that both the number and

437   osteogenic differentiation potential of bone marrow-derived MSCs decrease in osteoporotic

438   patients*(Xian L et al., 2012; Guan M et al., 2012)*. In our experiments, we found that iron caused

439   a concentration-dependent inhibitory effect of the viability of bone marrow-derived MSCs.

440   Furthermore, iron overload in bone marrow-derived MSCs result in increased apoptosis. This is

441   similar to our results in osteoblasts and also consistent with previous reports *(Chai X et al., 2015;*

442   *Zhang Y et al., 2015; Lu W et al., 2013)*. To explore the effect of iron-overload on the osteogenic

443   differentiation of bone marrow-derived MSCs, we estimated the change of ALP activity. In

444   response to osteogenic induction, bone marrow-derived MSCs could increase the activity of ALP,

445   a specific marker of osteogenic differentiation. In iron-overload condition, this response was

446   significantly attenuated. In addition, iron could directly inhibit matrix mineralization of bone

447   marrow-derived MSCs. Numerous clinical and in vivo studies have also indicated that defective

448   mineralization of bone was one of the pathological changes in iron overload-related

449   osteoporosis*(Doyard M et al., 2016; Mahachoklertwattana P et al., 2003; Matsushima S et al.,*

450   *2003).* Our in vitro findings that excess iron caused MSCs apoptosis and impaired osteogenic

451   differentiation and mineralization might ,at least in part, offer understanding of low bone density

452   in iron overload diseases.

453   Overall, our data indicate that iron significantly induces apoptosis in osteoblasts in vitro.

454   NAC could remarkably relieve iron overload-induced osteoblasts apoptosis. In addition, we

455   demonstrate that iron induces apoptosis via the enhanced production of ROS, which impairs

456   mitochondrial function and leads to MMP collapse, cytochrome c release, and caspase activation.

457   This provides valuable insights into the molecular mechanisms underlying osteoblastic cell death

458   in the iron-overload condition. Meanwhile, we also revealed that iron overload could promote

459   apoptosis and impair osteogenic differentiation and mineralization in bone marrow-derived

460   MSCs.

461   **Acknowledgments**

462   None.

463   **References**

464   ■ Vogiatzi MG, Macklin EA, Fung EB, Vichinsky E, Olivieri N, Kwiatkowski J, Cohen A,

465   Neufeld E, Giardina PJ. 2006. Prevalence of fractures among the Thalassemia syndromes in

466   North America. Bone. Apr;38(4):571-5. Epub 2005 Nov 17.

467   ■ Vogiatzi MG, Macklin EA, Fung EB, Cheung AM, Vichinsky E, Olivieri N, Kirby M,

468   Kwiatkowski JL, Cunningham M, Holm IA, Lane J, Schneider R, Fleisher M,Grady RW,

469   Peterson CC, Giardina PJ; Thalassemia Clinical Research Network. 2009 Bone disease in

470   thalassemia: a frequent and still unresolved problem. J Bone Miner Res. Mar;24(3):543-57.

471   doi: 10.1359/jbmr.080505.

472   ■ Kim BJ, Ahn SH, Bae SJ, Kim EH, Lee SH, Kim HK, Choe JW, Koh JM, Kim GS. 2012

473   Iron overload accelerates bone loss in healthy postmenopausal women and middle-aged

474   men:3-yearretrospective longitudinal study. J Bone Miner Res. Nov;27(11):2279-90. doi:

475   10.1002/jbmr.1692.

476   ■ Wong P, Fuller PJ, Gillespie MT, Kartsogiannis V, Kerr PG, Doery JC, Paul E, Bowden DK,

477   Strauss BJ, Milat F. 2014 Thalassemia bone disease: a 19-year longitudinal analysis. J Bone

478   Miner Res. Nov;29(11):2468-73. doi: 10.1002/jbmr.2266.

479   ■ Yang Q, Jian J, Abramson SB, Huang X. 2011 Inhibitory effects of iron on bone

480   morphogenetic protein 2-induced osteoblastogenesis. J Bone Miner Res. Jun;26(6):1188-96.

481   doi: 10.1002/jbmr.337.

482 ■ Tsay J, Yang Z, Ross FP, Cunningham-Rundles S, Lin H, Coleman R, Mayer-Kuckuk P,

483   Doty SB, Grady RW, Giardina PJ, Boskey AL, Vogiatzi MG. 2010. Bone loss caused by

484   iron overload in a murine model: importance of oxidative stress.Blood. 7;116(14):2582-9.

485   doi: 10.1182/blood-2009-12-260083.

486 ■ Messer JG, Kilbarger AK, Erikson KM, Kipp DE. 2009. Iron overload alters iron-regulatory

487   genes and proteins, down-regulates osteoblastic phenotype,and is associated with apoptosis

488   in fetal rat calvaria cultures. Bone ;45(5):972-9. doi: 10.1016/j.bone.2009.07.073.

489 ■ Doyard M, Fatih N, Monnier A, Island ML, Aubry M, Leroyer P, Bouvet R, Chalès G,

490   Mosser J, Loréal O, Guggenbuhl P. 2012. Iron excess limits HHIPL-2 gene expression and

491   decreases osteoblastic activity in human MG-63 cells. Osteoporos Int. Oct;23(10):2435-45.

492   doi: 10.1007/s00198-011-1871-z.

493 ■ Meng J, Ma X, Wang N, Jia M, Bi L, Wang Y, Li M, Zhang H, Xue X, Hou Z, Zhou Y, Yu

494   Z, He G, Luo X. 2016. Activation of GLP-1 Receptor Promotes

495   Bone Marrow Stromal Cell Osteogenic Differentiation through β-Catenin.

496   Stem Cell Reports. Apr 12;6(4):633. doi: 10.1016/j.stemcr.2016.03.010.

497 ■ Fuchs Y, Steller H. Programmed cell death in animal development and disease. 2011. Cell.

498   Nov 11;147(4):742-58. doi: 10.1016/j.cell.2011.10.033.

499 ■ Kroemer G, Galluzzi L, Brenner C. Mitochondrial membrane permeabilization in cell death.

500   2007. Physiol Rev. Jan;87(1):99-163.

501 ■ Green DR, Galluzzi L, Kroemer G. Cell biology. Metabolic control of cell death. 2014.

502   Science. Sep 19;345(6203):1250256. doi: 10.1126/science.1250256.

503 ■ Tait SW, Green DR. 2013. Mitochondrial regulation of cell death. Cold Spring Harb

504   Perspect Biol. Sep 1;5(9). pii: a008706. doi: 10.1101/cshperspect.a008706.

505 ■ Lill R. 2009. Function and biogenesis of iron-sulphur proteins. Nature. Aug

506   13;460(7257):831-8. doi: 10.1038/nature08301.

507 ■ Dixon SJ, Stockwell BR. 2014. The role of iron and reactive oxygen species in cell death.

508   Nat Chem Biol. Jan;10(1):9-17. doi: 10.1038/nchembio.1416.

509 ■ Pietrangelo A. 2016. Mechanisms of iron hepatotoxicity. J Hepatol. Feb 5. pii: S0168-

510   8278(16)00080-5. doi: 10.1016/j.jhep.2016.01.037.

511 ■ Zarjou A, Jeney V, Arosio P, Poli M, Zavaczki E, Balla G, Balla J. 2010. Ferritin

512   ferroxidase activity: a potent inhibitor of osteogenesis. J Bone Miner Res. Jan;25(1):164-72.

513   doi: 10.1359/jbmr.091002.

514 ■ Ding F, Shao ZW, Yang SH, Wu Q, Gao F, Xiong LM. 2012. Role of mitochondrial

515   pathway in compression-induced apoptosis of nucleus pulposus cells.

516   Apoptosis;17:579e90.18.

517 ■ Cai XY, Xia Y, Yang SH, Liu XZ, Shao ZW, Liu YL, Yang W, Xiong LM. 2015.

518   Ropivacaine- and bupivacaine-induced death of rabbit annulus fibrosus cells in vitro:

519   involvement of the mitochondrial apoptotic pathway. Osteoarthritis Cartilage.

520   Oct;23(10):1763-75. doi: 10.1016/j.joca.2015.05.013.

521 ■ Henry CM, Hollville E, Martin SJ. 2013. Measuring apoptosis by microscopy and flow

522   cytometry. Methods. Jun 1;61(2):90-7. doi: 10.1016/j.ymeth.2013.01.008.

523 ■ Zhu Y, Mao Z, Gao C. 2013. Control over the gradient differentiation of rat

524   BMSCs on a PCL membrane with surface-immobilized alendronate gradient.

525   Biomacromolecules. Feb 11;14(2):342-9. doi: 10.1021/bm301523p.

526 ■ Zhang X, Li J, Nie J, Jiang K, Zhen Z, Wang J, Shen L. 2010. Differentiation

527   character of adult mesenchymal stem cells and transfection of MSCs

528   withlentiviral vectors. J Huazhong Univ Sci Technolog Med Sci. Dec;30(6):687-93. doi:

529   10.1007/s11596-010-0641-z.

530 ■ Malladi P, Xu Y, Chiou M, Giaccia AJ, Longaker MT. 2006. Effect of reduced

531   oxygen tension on chondrogenesis and osteogenesis in adipose-derived   mesenchymal cells.

532   Am J Physiol Cell Physiol. Apr;290(4):C1139-46.

533 ■ Lyu Z, Wang H, Wang Y, Ding K, Liu H, Yuan L, Shi X, Wang M, Wang Y, Chen H. 2014.

534 Maintaining the pluripotency of mouse embryonic stem cells on gold nanoparticle layers

535 with nanoscale but not microscale surface roughness. Nanoscale. Jun 21;6(12):6959-69. doi:

536 10.1039/c4nr01540a.

537 ■ Tenopoulou M, Kurz T, Doulias PT, Galaris D, Brunk UT. 2007. Does the calcein-AM

538 method assay the total cellular 'labile iron pool' or only a fraction of it? Biochem J. Apr

539 15;403(2):261-6.

540 ■ Glickstein H, El RB, Shvartsman M, Cabantchik ZI. 2005. Intracellular labile iron pools as

541 direct targets of iron chelators: fluorescence study of chelator action in livingcells. Blood.

542 Nov 1;120(9):3242-50.

543 ■ Kaur D, Lee D, Ragapolan S, Andersen JK. 2009. Glutathione depletion in immortalized

544 midbrain-derived dopaminergic neurons results in increases in the labile iron pool:

545 implications for Parkinson's disease. Free Radic Biol Med. Mar 1;46(5):593-8. doi:

546 10.1016/j.freeradbiomed.2008.11.012.

547 ■ Brissot P, Ropert M, Le Lan C, Loréal O. 2012. Non-transferrin bound iron: a key role in

548 iron overload and iron toxicity. Biochim Biophys Acta. Mar;1820(3):403-10. doi:

549 10.1016/j.bbagen.2011.07.014.

550 ■ Wong P, Fuller PJ, Gillespie MT, Kartsogiannis V, Strauss BJ, Bowden D, Milat F. 2013.

551 Thalassemia bone disease: the association between nephrolithiasis, bone mineral density and

552   fractures. Osteoporos Int. Jul;24(7):1965-71. doi: 10.1007/s00198-012-2260-y.

553   ■ Haidar R, Musallam KM, Taher AT. 2011. Bone disease and skeletal complications in

554   patients with β thalassemia major. Bone. Mar 1;48(3):425-32. doi:

555   10.1016/j.bone.2010.10.173.

556   ■ Valenti L, Varenna M, Fracanzani AL, Rossi V, Fargion S, Sinigaglia L. 2009. Association

557   between iron overload and osteoporosis in patients with hereditary hemochromatosis.

558   Osteoporos Int. Apr;20(4):549-55. doi: 10.1007/s00198-008-0701-4.

559   ■ Li GF, Pan YZ, Sirois P, Li K, Xu YJ. 2012. Iron homeostasis in osteoporosis and its clinical

560   implications. Osteoporos Int. Oct;23(10):2403-8. doi: 10.1007/s00198-012-1982-1.

561   ■ Fiona Mitchell. 2012. Bone: High body iron stores lead to bone loss. Nature Reviews

562   Endocrinology 8, 506 (September) | doi:10.1038/nrendo.2012.127

563   ■ Domrongkitchaiporn S, Sirikulchayanonta V, Angchaisuksiri P, Stitchantrakul W,

564   Kanokkantapong C, Rajatanavin R. 2003. Abnormalities in bone mineral density and bone

565   histology in thalassemia. J Bone Miner Res. Sep;18(9):1682-8.

566   ■ Terpos E, Voskaridou E. 2010. Treatment options for thalassemia patients with osteoporosis.

567   Ann N Y Acad Sci. Aug;1202:237-43.

568   ■ Mahachoklertwattana P, Sirikulchayanonta V, Chuansumrit A, Karnsombat P, Choubtum L,

569   Sriphrapradang A, Domrongkitchaiporn S, Sirisriro R, Rajatanavin R. 2003. Bone

570   histomorphometry in children and adolescents with beta-thalassemia disease: iron-associated

571   focal osteomalacia. J Clin Endocrinol Metab. Aug;88(8):3966-72.

572 ■ Doyard M, Chappard D, Leroyer P, Roth MP, Loréal O, Guggenbuhl P. 2016. Decreased

573   Bone Formation Explains Osteoporosis in a Genetic Mouse Model of

574   Hemochromatosiss.PLoS One. Feb 1;11(2):e0148292.

575 ■ Esposito BP, Breuer W, Sirankapracha P, Pootrakul P, Hershko C, Cabantchik ZI. 2003.

576   Labile plasma iron in iron overload: redox activity and susceptibility to chelation. Blood.

577   Oct 1;102(7):2670-7.

578 ■ Devos D, Moreau C, Devedjian JC, Kluza J, Petrault M, Laloux C, Jonneaux A, Ryckewaert

579   G, Garçon G, Rouaix N, Duhamel A, Jissendi P, Dujardin K, Auger F,Ravasi L, Hopes L,

580   Grolez G, Firdaus W, Sablonnière B, Strubi-Vuillaume I, Zahr N, Destée A, Corvol JC, Pöltl

581   D, Leist M, Rose C, Defebvre L, Marchetti P,Cabantchik ZI, Bordet R. 2014. Targeting

582   chelatable iron as a therapeutic modality in Parkinson's disease. Antioxid Redox Signal. Jul

583   10;21(2):195-210. doi: 10.1089/ars.2013.5593.

584 ■ Berdoukas V, Coates TD, Cabantchik ZI. 2015. Iron and oxidative stress in cardiomyopathy

585   in thalassemia. Free Radic Biol Med. Nov;88(Pt A):3-9. doi:

586   10.1016/j.freeradbiomed.2015.07.019.

587 ■ Chai X, Li D, Cao X, Zhang Y, Mu J, Lu W, Xiao X, Li C, Meng J, Chen J, Li Q, Wang J,

588   Meng A, Zhao M. 2015. ROS-mediated iron overload injures the hematopoiesis of bone

589   marrow by damaging hematopoietic stem/progenitor cells in mice. Sci Rep. May 13;5:10181.

590   doi: 10.1038/srep10181.

591 ■ Sahoo S, Meijles DN, Pagano PJ. 2016. NADPH oxidases: key modulators in aging and age-

592   related cardiovascular diseases? Clin Sci (Lond). Mar 1;130(5):317-35. doi:

593   10.1042/CS20150087.

594 ■ Dikalov S. 2011. Cross talk between mitochondria and NADPH oxidases. Free Radic Biol

595   Med.1;51(7):1289-301. doi: 10.1016/j.freeradbiomed.2011.06.033.

596 ■ Zhou J, Ye S, Fujiwara T, Manolagas SC, Zhao H. 2013. Steap4 plays a critical role in

597   osteoclastogenesis in vitro by regulating cellular iron/reactive oxygen species (ROS) levels

598   and cAMP response element-binding protein (CREB) activation. J Biol Chem. Oct

599   18;288(42):30064-74. doi: 10.1074/jbc.M113.478750.

600 ■ Manolagas SC. 2010. From estrogen-centric to aging and oxidative stress: a revised

601   perspective of the pathogenesis of osteoporosis. Endocr Rev. Jun;31(3):266-300. doi:

602   10.1210/er.2009-0024.

603 ■ Schröder K. 2015. NADPH oxidases in bone homeostasis and osteoporosis. Cell Mol Life

604   Sci. Jan;72(1):25-38. doi: 10.1007/s00018-014-1712-2.

605 ■ Bedard K, Krause KH. 2007. The NOX family of ROS-generating NADPH oxidases:

606   physiology and pathophysiology. Physiol Rev. Jan;87(1):245-313.

607 ■ Chan S, yu Ye J, Chan G C F. 2013. TPO exerts a protective effect on iron-overload induces

608   apoptosis in cardiomyocytes via mitochondrial pathways. Blood, 122(21): 4668-4668.

609 ■ Park J, Lee DG, Kim B, Park SJ, Kim JH, Lee SR, Chang KT, Lee HS, Lee DS. 2015. Iron

610   overload triggers mitochondrial fragmentation via calcineurin-sensitive signals in HT-22

611   hippocampal neuron cells. Toxicology. Nov 4;337:39-46. doi: 10.1016/j.tox.2015.08.009.

612 ■ Dussiot M, Maciel TT, Fricot A, Chartier C, Negre O, Veiga J, Grapton D, Paubelle E,

613   Payen E, Beuzard Y, Leboulch P, Ribeil JA, Arlet JB, Coté F, Courtois G, Ginzburg YZ,

614   Daniel TO, Chopra R, Sung V, Hermine O, Moura IC. 2014. An activin receptor IIA ligand

615   trap corrects ineffective erythropoiesis in β-thalassemia. Nat Med. Apr;20(4):398-407. doi:

616   10.1038/nm.3468.

617 ■ Chen MP, Cabantchik ZI, Chan S, Chan GC, Cheung YF. 2014 Iron overload and apoptosis

618   of HL-1 cardiomyocytes: effects of calcium channel blockade. PLoS One. 12;9(11):e112915.

619   doi: 10.1371/journal.pone.0112915. eCollection 2014.

620 ■ Sripetchwandee J, KenKnight SB, Sanit J, Chattipakorn S, Chattipakorn N. 2014. Blockade

621   of mitochondrial calcium uniporter prevents cardiac mitochondrial dysfunction caused by

622   iron overload. Acta Physiol (Oxf). Feb;210(2):330-41. doi: 10.1111/apha.12162.

623 ■ Pelizzoni I, Macco R, Morini MF, Zacchetti D, Grohovaz F, Codazzi F. 2011. Iron handling

624   in hippocampal neurons: activity-dependent iron entry andmitochondria-mediated

625   neurotoxicity. Aging Cell. Feb;10(1):172-83. doi: 10.1111/j.1474-9726.2010.00652.x.

626 ■ Uchiyama A, Kim JS, Kon K, Jaeschke H, Ikejima K, Watanabe S, Lemasters JJ. 2008.

627 Translocation of iron from lysosomes into mitochondria is a key event during oxidative

628 stress-induced hepatocellular injury. Hepatology. Nov;48(5):1644-54. doi:

629 10.1002/hep.22498.

630 ■ Ward RJ, Zucca FA, Duyn JH, Crichton RR, Zecca L. 2014. The role of iron in brain ageing

631 and

632 neurodegenerative disorders. Lancet Neurol. Oct;13(10):1045-60.

633 doi:10.1016/S1474-4422(14)70117-6.

634 ■ Mallikarjun V, Sriram A, Scialo F, Sanz A. 2014. The interplay between mitochondrial

635 protein and iron homeostasis and its possible role in ageing. Exp Gerontol. Aug;56:123-34.

636 doi: 10.1016/j.exger.2013.12.015.

637 ■ Al-Qenaei A, Yiakouvaki A, Reelfs O, Santambrogio P, Levi S, Hall ND, Tyrrell RM,

638 Pourzand C. 2014. Role of intracellular labile iron, ferritin, and antioxidant defence in

639 resistance of chronically adapted Jurkat T cells to hydrogen peroxide. Free Radic Biol Med.

640 Mar;68:87-100. doi: 10.1016/j.freeradbiomed.2013.12.006.

641 ■ Santambrogio P, Dusi S, Guaraldo M, Rotundo LI, Broccoli V, Garavaglia B, Tiranti V,

642 Levi S. 2015. Mitochondrial iron and energetic dysfunction distinguish fibroblasts and

643 induced neurons from pantothenatekinase-associated neurodegeneration patients. Neurobiol

644 Dis. Sep;81:144-53. doi: 10.1016/j.nbd.2015.02.030.

645 ■ Rouault TA. 2016. Mitochondrial iron overload: causes and consequences. Curr Opin Genet

646   Dev.Mar 25;38:31-37. doi: 10.1016/j.gde.2016.02.004.

647 ■ Rines AK, Ardehali H. 2013. Transition metals and mitochondrial metabolism in the heart. J

648   Mol Cell Cardiol. Feb;55:50-7. doi: 10.1016/j.yjmcc.2012.05.014.

649 ■ Czabotar PE, Lessene G, Strasser A, Adams JM. 2014. Control of apoptosis by the BCL-2

650   protein family: implications for physiology and therapy. Nat Rev Mol Cell Biol.

651   Jan;15(1):49-63. doi: 10.1038/nrm3722.

652 ■ Hardwick JM, Soane L. 2013. Multiple functions of BCL-2 family proteins. Cold Spring

653   Harb Perspect Biol. Feb 1;5(2). pii: a008722. doi: 10.1101/cshperspect.a008722.

654 ■ Yamada M, Tsukimura N, Ikeda T, Sugita Y, Att W, Kojima N, Kubo K, Ueno T, Sakurai K,

655   Ogawa T. 2013. N-acetyl cysteine as an osteogenesis-enhancing molecule for bone

656   regeneration. Biomaterials. Aug;34(26):6147-56. doi: 10.1016/j.biomaterials.2013.04.064.

657 ■ Jun JH, Lee SH, Kwak HB, Lee ZH, Seo SB, Woo KM, Ryoo HM, Kim GS, Baek JH. 2008.

658   N-acetylcysteine stimulates osteoblastic differentiation of mouse calvarial cells. J Cell

659   Biochem. Mar 1;103(4):1246-55.

660 ■ Hyeon S, Lee H, Yang Y, Jeong W. 2013. Nrf2 deficiency induces oxidative stress and

661   promotes RANKL-inducedosteoclast differentiation. Free Radic Biol Med. 65:789-99. doi:

662   10.1016/j.freeradbiomed.2013.08.005.

663 ■ Lee NK, Choi YG, Baik JY, Han SY, Jeong DW, Bae YS, Kim N, Lee SY. 2005. A crucial

664 role for reactive oxygen species in RANKL-induced osteoclastdifferentiation. Blood. Aug

665 1;120(3):852-9.

666 ■ Czekanska EM, Stoddart MJ, Richards RG, Hayes JS. 2012. In search of an osteoblast cell

667 model for in vitro research. Eur Cell Mater. Jul 9;24:1-17.

668 ■ Ma KG, Shao ZW, Yang SH, Wang J, Wang BC, Xiong LM, Wu Q, Chen SF. Autophagy is

669 activated in compression-induced cell degeneration and is mediated by reactive oxygen

670 species innucleus pulposus cells exposed to compression. Osteoarthritis Cartilage. 2013

671 Dec;21(12):2030-8. doi: 10.1016/j.joca.2013.10.002.

672 ■ Xian L, Wu X, Pang L, Lou M, Rosen CJ, Qiu T, Crane J, Frassica F, Zhang L, Rodriguez

673 JP, Xiaofeng Jia, Shoshana Yakar, Shouhong Xuan, Argiris Efstratiadis, Mei Wan, Xu Cao.

674 2012. Matrix IGF-1 maintains bone mass by activation of mTOR in mesenchymal stem cells.

675 Nat Med. Jul;18(7):1095-101. doi: 10.1038/nm.2793.

676 ■ Guan M, Yao W, Liu R, Lam KS, Nolta J, Jia J, Panganiban B, Meng L, Zhou P, Shahnazari

677 M, Ritchie RO, Lane NE. 2012. Directing mesenchymal stem cells to bone to augment bone

678 formation and increase bone mass. Nat Med. Feb 5;18(3):456-62. doi: 10.1038/nm.2665.

679 ■ Zhang Y, Zhai W, Zhao M, Li D, Chai X, Cao X, Meng J, Chen J, Xiao X, Li Q, Mu J, Shen

680 J, Meng A. 2015. Effects of iron overload on the bone marrow

681 microenvironment in mice. PLoS One. Mar 16;10(3):e0120219. doi:

682   10.1371/journal.pone.0120219.

683   ■ Mahachoklertwattana P, Sirikulchayanonta V, Chuansumrit A, Karnsombat P, Choubtum

684   L, Sriphrapradang A, Domrongkitchaiporn S, Sirisriro R,Rajatanavin R. 2003. Bone

685   histomorphometry in children and adolescents with beta-thalassemia disease: iron-associated

686   focal osteomalacia. J Clin Endocrinol Metab. Aug;88(8):3966-72.

687   ■ Matsushima S, Torii M, Ozaki K, Narama I. 2003. Iron lactate-induced osteomalacia in

688   association with osteoblast dynamics. Toxicol Pathol. Nov-Dec;31(6):646-54.

689   ■ Lu W, Zhao M, Rajbhandary S, Xie F, Chai X, Mu J, Meng J, Liu Y, Jiang Y, Xu X, Meng

690   A. 2013. Free iron catalyzes oxidative damage to hematopoietic

691   cells/mesenchymal stem cells in vitro and suppresses hematopoiesis in iron overload patients.

692   Eur J Haematol. Sep;91(3):249-61. doi: 10.1111/ejh.12159.
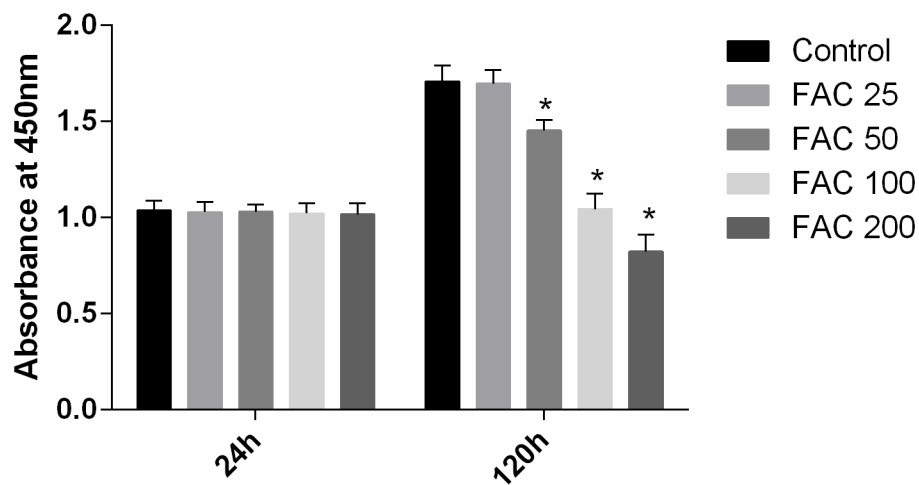
693

694

695

696

697

698

699

700

701

702

703   **Figure 1 Cytotoxic effects of iron on the viability of osteoblasts.**

704   Viability of osteoblasts was evaluated by CCK-8 assay after treatment with FAC (25-200 μM) for 24

705   h and 120 h. Compared to the control (FAC 0 μM), iron significantly reduced cell viability after 120-

706   h FAC treatment. The values are presented as means ± SD, n = 3; *P < 0.05 vs. the control.
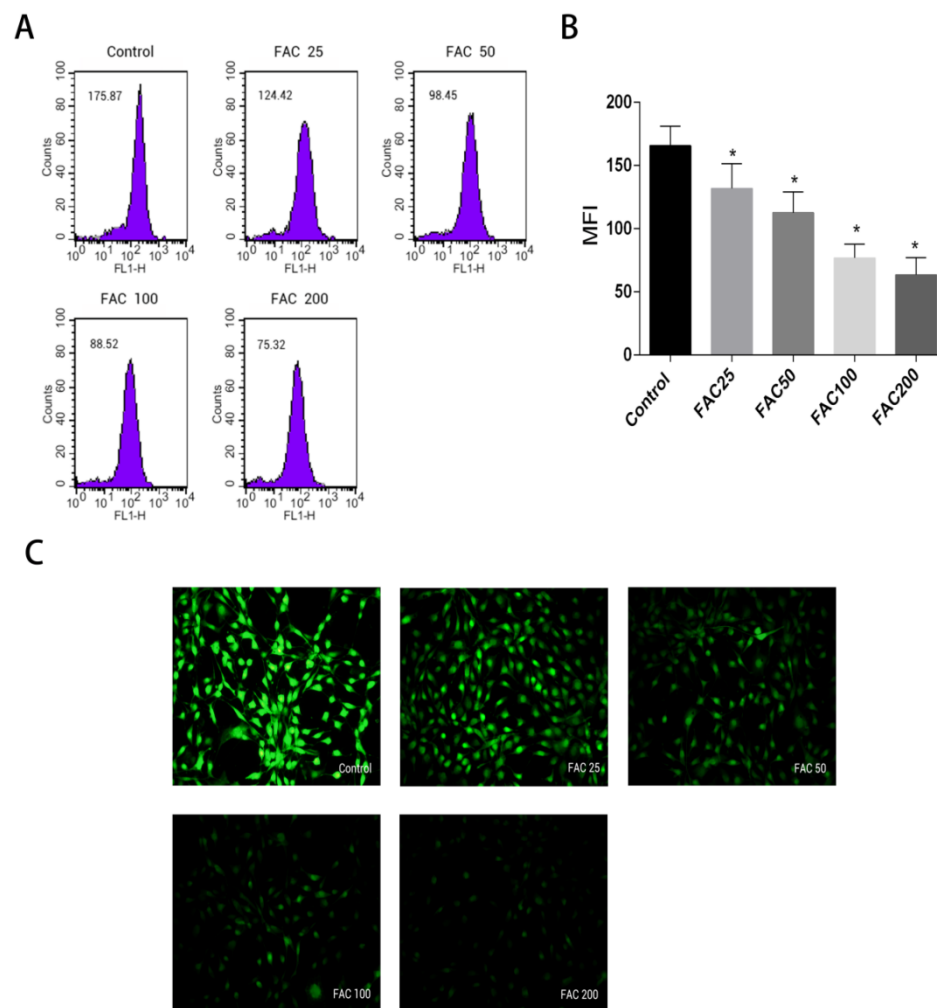
Figure 2 Effect of iron-overload on the intracellular LIP in osteoblasts.

The intracellular LIP in osteoblasts markedly increased after treatment with 0-200 μM FAC for 120 h.

(A) Representative flow cytometric results for intracellular LIP after FAC treatment. The intracellular

LIP was estimated by calcein-AM, a fluorescent iron-sensitive probe. The probe fluorescence was

quenched after chelating with labile iron; the mean fluorescence intensity (MFI) measured by flow

cytometry was negatively correlated with intracellular LIP. (B) The reduction in MFI indicated an

elevation in the intracellular LIP in the osteoblasts. Data are presented as the means ± SD, n = 3; *P <

715   0.05 vs. the control. (C) Representative fluorescence microscopy photomicrographs of intracellular

716   LIP in osteoblasts. The quenching of green fluorescence indicates that the intracellular LIP was

717   increased in cells.

718
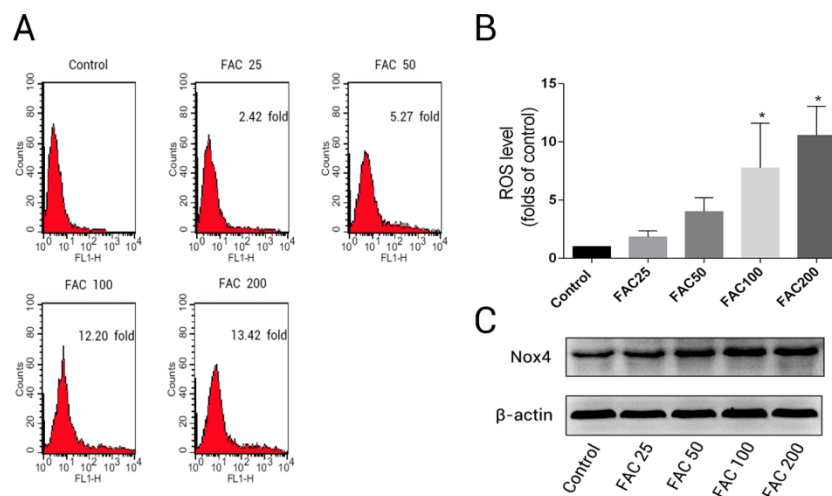
719   **Figure 3 Iron induced ROS generation and upregulation of Nox4 in osteoblasts.**

720   (A) Representative data of flow cytometric measurement of ROS production after labeling with

721   H2DCF-DA. (B) Statistical bar graphs show the ROS levels in osteoblasts. The fluorescence intensity

722   of osteoblasts was expressed relative to untreated osteoblasts (FAC 0 μM). Date are presented as

723   means ± SD, n = 3 ;*P < 0.05 vs. the control. (C) Representative western blot data for Nox4 in

724   osteoblasts following exposure to FAC(0-200 μM) for 120 h. GAPDH was used as an internal control.

725
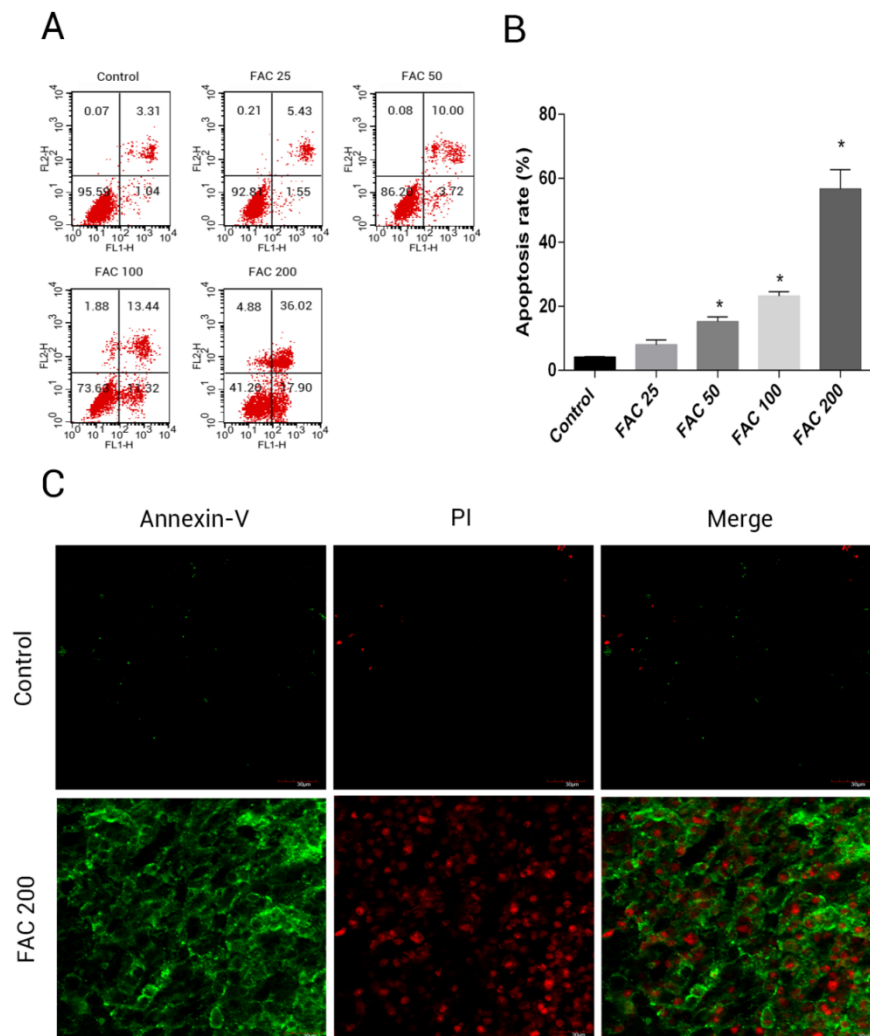
Figure 4 Iron induced apoptosis in osteoblasts.

(A) Representative flow cytometric analysis of apoptotic osteoblasts stained for Annexin V/PI after

exposure to 0-200 µM FAC for 120 h. In each plot, the lower left quadrant represents live osteoblasts,

the lower right and upper right quadrants represent apoptotic osteoblasts, and the upper left quadrant

represents necrotic osteoblasts. (B) Statistical bar graphs show the mean values of flow cytometry

data. Data are presented as the means ± SD, n = 3. *P < 0.05 vs. the control. (C) Representative

photomicrograph (OLYMPUS FV1000, Japan) of osteoblasts stained with AnnexinV/PI dye after

733   treatment with 0 μM and 200 μM FAC for 120 h. Apoptotic osteoblasts were defined as annexin-V+/

734   PI- cells and annexin-V+/PI- cells.
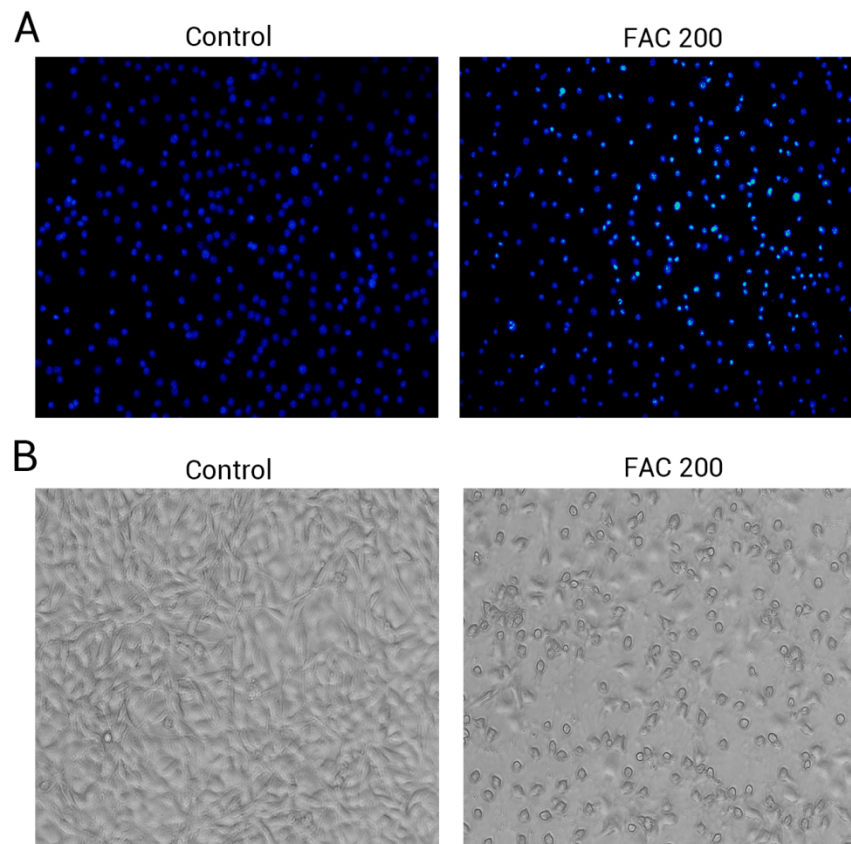
736   **Figure 5 The morphological changes of apoptosis in osteoblasts FAC.**

737   (A) Hoechst 33258 staining of osteoblasts after treatment with PBS (Control) and 200 μM FAC (FAC

738   200) for 120 h. Apoptotic osteoblasts showed condensed and bright nuclei stained by Hoechst 33258.

739   (B) Phase-contrast photomicrograph of osteoblasts after treatment with PBS (Control) and 200 μM

740   FAC (FAC 200) for 120 h. Apoptotic osteoblasts presented shrinkage and swelling and detached

741   from the plates.

742

743
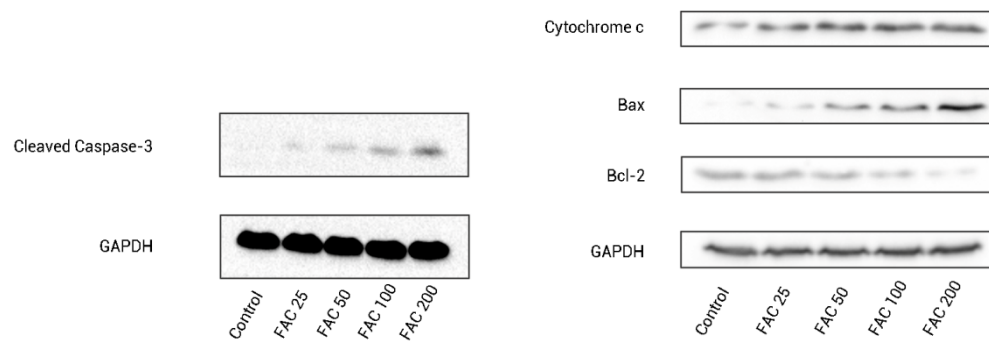
Figure 6 The expression of apoptosis-related proteins in osteoblasts.

Representative western blot data for cleaved Caspase-3, Bax, Bcl-2, and cytosolic cytochrome c in

osteoblasts following exposure to FAC(0-200 µM) for 120 h. GAPDH was used as an internal control.

A

B

C

747
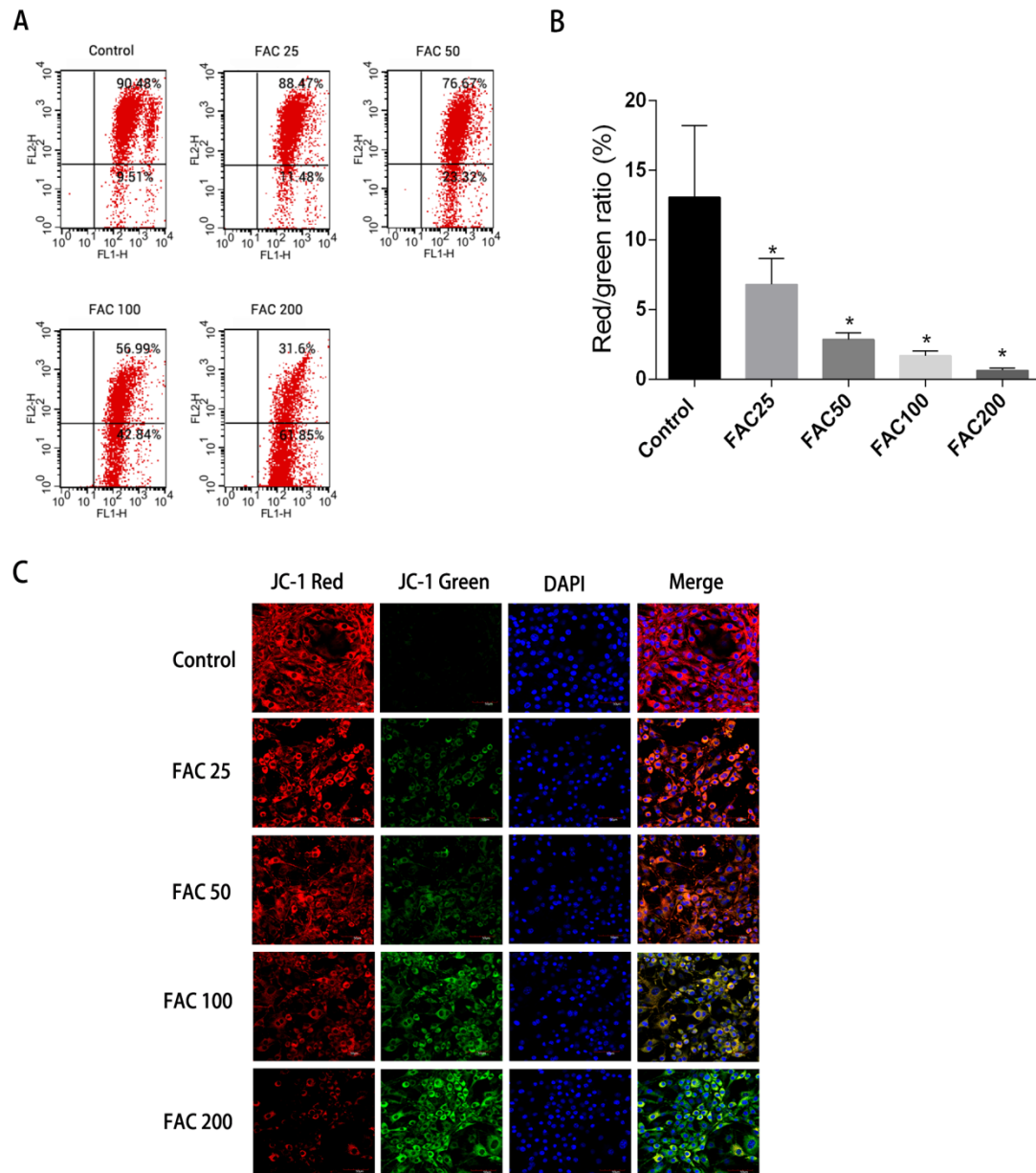
Figure 7 Iron-induced decrease in MMP of osteoblasts.

749   The MMP in osteoblasts treated with FAC (0-200 μM) for 120 h as measured by JC-1 staining. (A)

750   Representative graphs of flow cytometric analysis of the altered MMP after incubating with JC-1 dye.

751   (B) Statistical bar graphs show the changes of MMP detected by flow cytometry. The changes of

752   MMP in osteoblasts were defined as the ratio of red/green fluorescence intensity. Data are presented

753   as the means ± SD, n = 3. *P < 0.05 vs. the control. (C) Representative laser scan confocal

754   microscopy photomicrographs of osteoblasts stained with JC-1 dye.

755
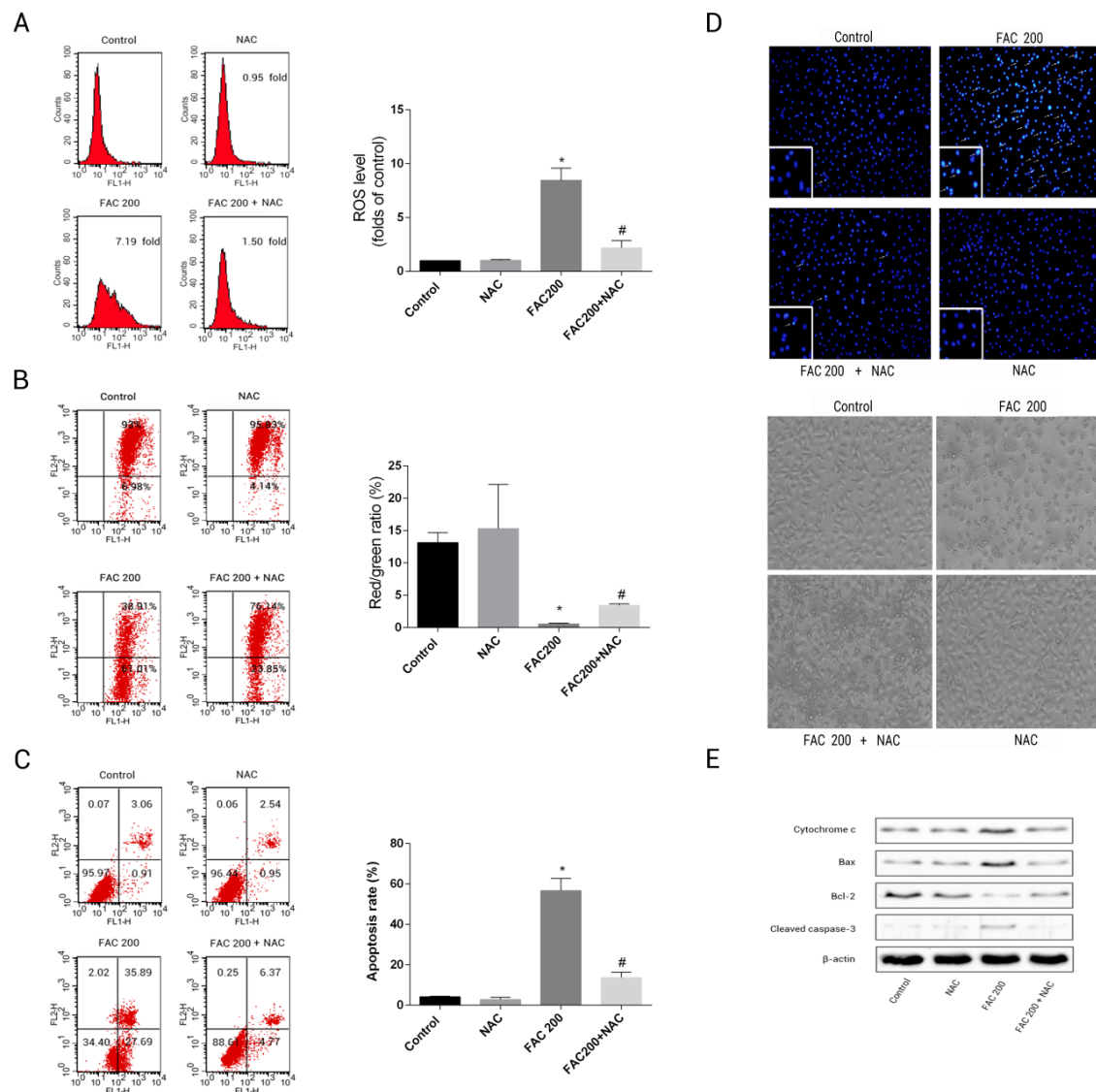
756   **Figure 8 Protective effects of NAC against iron-induced apoptosis.**

757   Osteoblasts were exposed to FAC (200 μM) with or or without NAC (1 mM) for 120 h. (A) The

758   change of intracellular ROS levels in osteoblasts   treated with FAC (200 μM) with or without NAC

759   (1mM) for 120 h. *P < 0.05 vs .the control ;   #P < 0.05 vs. FAC 200. (B) The change of MMP in

760   osteoblasts incubated wtih FAC (200 μM), in the absence or presence of 1 mM NAC for 120 h, as

761   assayed by flow cytometry. *P < 0.05 vs. the control ; #P < 0.05 vs. FAC 200. (C) The effect of NAC

762   on iron-induced cell apoptosis as assayed by flow cytometry analysis. *P < 0.05 vs. the control ; #P <

763   0.05 vs. FAC 200. (D) The effect of NAC on iron-induced morphological changes in cells as

764   visualized by phase-contrast micrograph and Hoechst 33342 staining. (E) The effect of NAC on the

765   expression of apoptosis-related proteins in iron-treated osteoblastic cells.

766
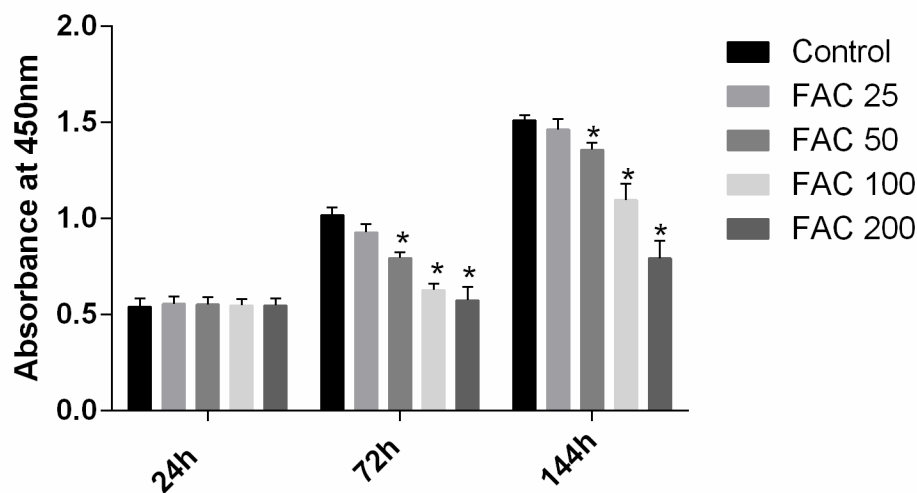
Figure 9 Cytotoxic effects of iron on the viability of bone marrow-derived MSCs.

768 Viability of bone marrow-derived MSCs was evaluated by CCK-8 assay after treatment with FAC

769 (25-200 μM) for 24 h, 72 h and 144 h. Compared to the control (FAC 0 μM), iron significantly

770 reduced cell viability after 72 h and 120 h FAC treatment. The values are presented as means ± SD, n

771 = 3; *P < 0.05 vs. the control.

772
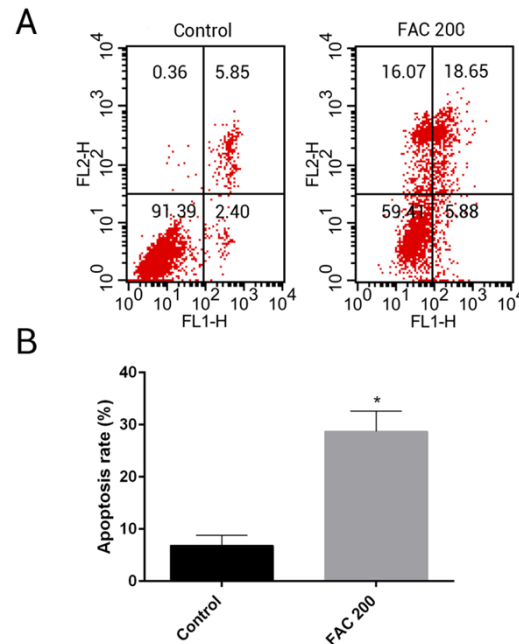
Figure 10 Iron induced apoptosis in bone marrow-derived MSCs.

(A) Representative flow cytometric analysis of apoptotic MSCs stained for Annexin V/PI after

exposure to 200 μM FAC for 144 h. In each plot, the lower left quadrant represents live MSCs, the

lower right and upper right quadrants represent apoptotic MSCs, and the upper left quadrant

represents necrotic MSCs. (B) Statistical bar graphs show the mean values of flow cytometry data.

Data are presented as the means ± SD, n = 3. *P < 0.05 vs. the control.

779
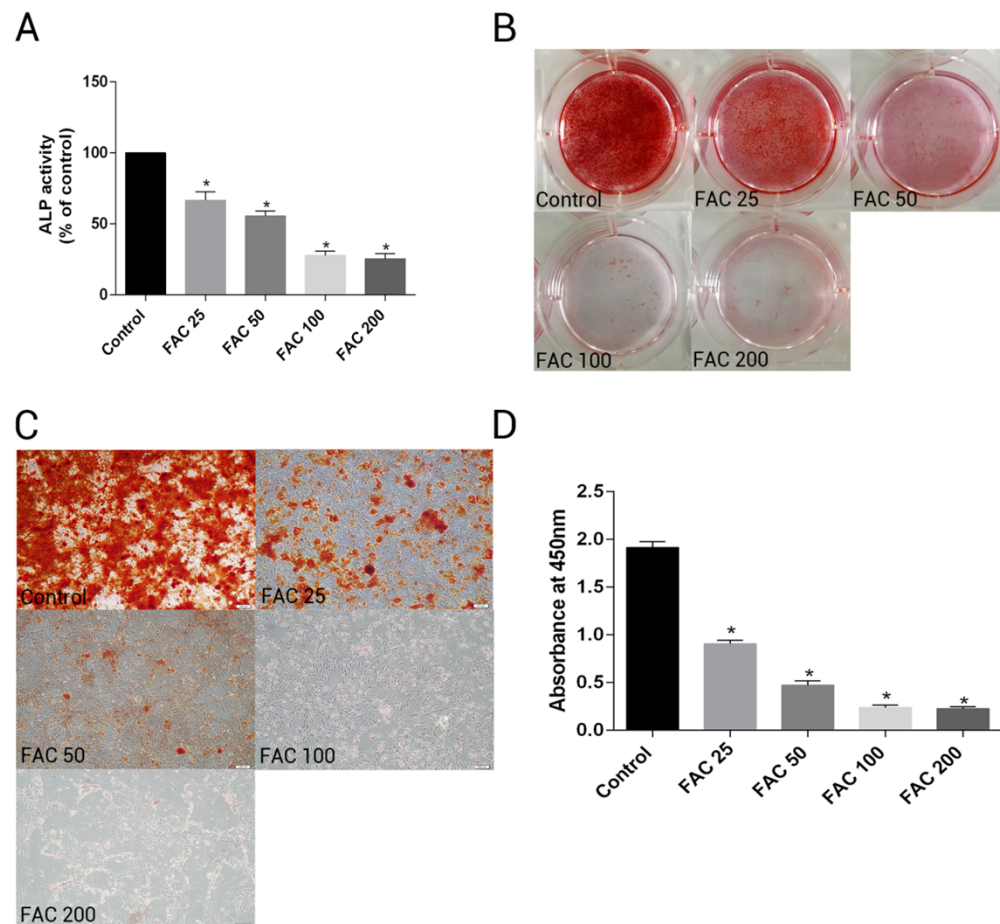
780 **Figure 11 Effect of iron on ALP activity and matrix calcification**

781 (A-D) Primary bone marrow-derived MSCs cultured in 6-well plates were induced with osteogenic

782 medium supplemented with FAC (25-200 μM) or alone for 14 d. (A) ALP activity of MSCs was

783 detected as described in Materials and Methods. Data are presented as the means ± SD, n = 3. *P <

784 0.05 vs. the control. (B-C) Mineralization in bone marrow-derived MSCs was assayed by Alizarin

785 Red staining. Representative photographic images of stained wells (B) and microscopic views(C) are

786 shown. (D) Statistical bar graphs show Ca content from different groups. Data are presented as the

787 means ± SD, n = 3. *P < 0.05 vs. the control.

788
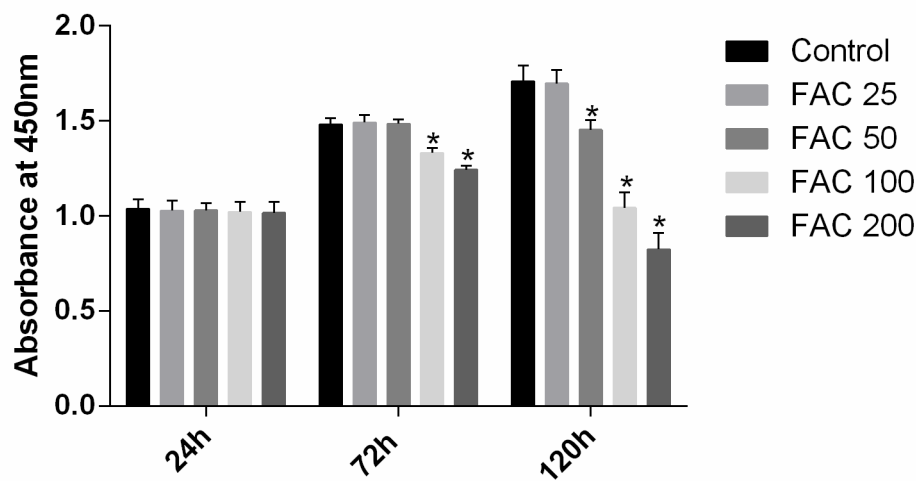
Supplementary Figure 1 Cytotoxic effects of iron on the viability of osteoblasts.

790   Viability of osteoblasts was evaluated by CCK-8 assay after treatment with FAC (25-200 μM) for 24

791   h, 72h and 120 h. Compared to the control (FAC 0 μM), iron significantly reduced cell viability in a

792   dose-dependent manner after 120-h FAC treatment. The values are presented as means ± SD, n = 3;

793   *P < 0.05 vs. the control.

794

795
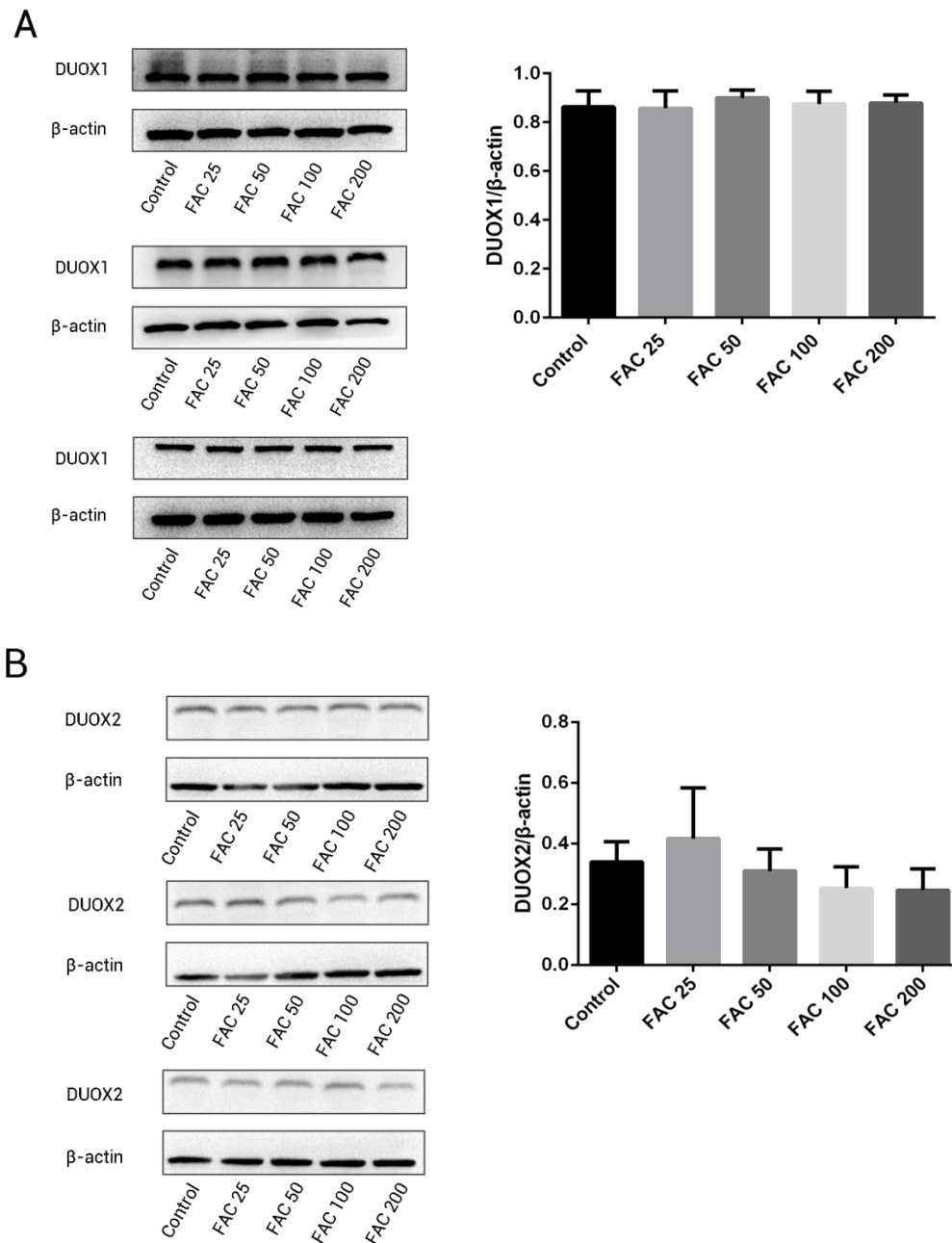
796 **Supplementary Figure 2 Effect of iron on the exprssion of DUOX1 and DUOX2 in**

797 **osteoblasts**

798 (A-B) Representative western blot data for DUOX1 and DUOX2 in osteoblasts following exposure to

799 FAC(0-200 μM) for 120 h. β -actin was used as an internal control. Date are presented as means ±

800   SD, n = 3 ;*P < 0.05 vs. the control.